

# Generator of QCD Parton Model for the Cosmic Ray Ultrahigh Energy Interaction

Cao Zhen and Ding Linkai

(Institute of High Energy Physics, Chinese Academy of Sciences, Beijing)

A parton model based on perturbative QCD is developed for the description of ultrahigh energy interaction between cosmic ray and air nuclei. A LLA QCD calculation of jet production cross section in proton-proton scattering and a hadronization scheme based on independent fragmentation model are presented. A number of parameters in the hadronization scheme are selected such that the basic features of hadronic production in  $e^+e^-$  collision covering C.M. energy region from 14 GeV to 91 GeV can be reproduced. A Monte Carlo generator is constructed to reproduce the basic characteristics of proton-antiproton scattering at the C.M. energy from 80 GeV to 1800 GeV and extended to ultrahigh energy region up to 22 TeV.

**Key words** ultrahigh energy interaction, QCD parton model, transverse momentum, pseudorapidity, hadronization,  $e^+e^-$  collision,  $p\bar{p}$ -scattering, jet.

---

## 1. INTRODUCTION

Emulsion chambers have been adopted to observe the air shower induced by ultrahigh energy cosmic rays for many years. The term "ultrahigh energy" means that the interaction energy between colliding particles is higher than that of current colliders, typically from  $10^{15}$  to  $10^{17}$  eV in the fixed target system. At such high energy, the cosmic ray entering the atmosphere interact with the air

---

Received on August 2, 1993.

© 1995 by Allerton Press, Inc. Authorization to photocopy individual items for internal or personal use, or the internal or personal use of specific clients, is granted by Allerton Press, Inc. for libraries and other users registered with the Copyright Clearance Center (CCC) Transactional Reporting Service, provided that the base fee of \$50.00 per copy is paid directly to CCC, 222 Rosewood Drive, Danvers, MA 01923. An annual license may be obtained only directly from Allerton Press, Inc., 150 5th Avenue, New York, NY 10011.

nucleus and induce cascades. The secondaries of the cascade can be recorded by the emulsion chambers installed on the quite high level of mountains with a quite high threshold energy, typically 4 TeV. As a nearly unique method of studying the ultrahigh energy strong interaction, cosmic ray emulsion chamber experiments obtained the reasonable results [1-3]. Two of the main results on the characters of the ultrahigh energy air shower cascade have been summarized as follows: the first is its fast attenuation in the atmosphere compared to that predicted by traditional models; the other is the existence of a multi-cluster structure in part of the gamma-families. The fast attenuation of the showers not only reflects the degree of the Feynman scaling violation in the interaction forward region and other properties of the ultrahigh energy interaction, but also strongly depends on the composition of the primary cosmic rays, which is unknown in the ultrahigh energy region so far. Various assumptions of the composition of cosmic rays have been introduced, based on these different assumptions. Even if there are rather large differences, various current models of the ultrahigh energy interaction can explain the fast attenuation as long as a suitable assumption of the composition of the primary cosmic rays is selected. In other words, we learned almost nothing from this character on the property of strong interaction at ultrahigh energies; however, the multi-cluster structures in part of the gamma families are found mainly in those families induced by cosmic ray protons [2, 4]. This means that the phenomenon is nearly independent of the assumption of primary cosmic ray composition, so this type of the phenomenon is expected to be more sensitive to the ultrahigh energy interaction property. Furthermore, the mechanism of the formation of the double or multi-cluster structure in the family is believed associating with the high  $p_T$  jet production in the ultrahigh energy interaction. The analyses of the double cluster phenomenon in the framework of perturbative chromodynamics (pQCD) is expected to be a possibility to test the standard model at ultrahigh energy, even to be a possibility to explore the signal of possible compositeness of quarks [5].

In fact, most of the families with typical double cluster structures have been explained with the models [2,4] based on pQCD jet production. However, there exist a few families with extremely large apparent transverse momentum [3] which cannot be explained by the prediction of those models. However, enormous data on  $p\bar{p}$  scatterings have been accumulated in the collider experiments, e.g., that on Sp $\bar{p}$ S and Tevatron, at slightly lower energies than in the cosmic ray emulsion chamber experiments. More detailed information about the hadronic structure obtained from the analyses of a bulk of data of deep inelastic scatterings and Drell-Yan processes. More accurate measurement of  $\alpha_s$  and the improvements of the models of the hadronization of partons have been achieved due to the  $e^+e^-$  colliding experiments at various energies, e.g., from a few GeV (TASSO) to 91 GeV (LEP). After all of those developments in the accelerator experiments, it is necessary to reinvestigate the double cluster phenomenon in the emulsion chamber cosmic ray experiments from a fresh viewpoint. Essentially, it is required to build a  $p\bar{p}$  interaction model based on the pQCD parton model, which can take new experimental data into account, comprehend new physics idea, e.g., the effects of the compositeness of quarks, higher twist correction (prompt high  $p_T$  directly meson production), etc.

Chromodynamics is the most probable candidate theory of the strong interaction. The application of QCD in various phenomenological problems for testing its correctness and exploring the new physics beyond it is one of the most important topics in high energy strong interaction physics. Perturbative QCD proves to be successful in describing such processes with sufficient large momentum transfer at the collider energies. The meaning of large momentum transfer here is well defined. For example, only the hard scattering between partons belongs to this category in the typical four jets production in a proton collision, whereas, the fragmentation of the beam and target jets, which carry the most of the energy of the proton colliding system, cannot be dealt with pQCD; instead, it has to be described in terms of the phenomenological soft hadronic interaction model because the momentum transfer in the fragmentation is too small. Additionally, the hadronization of the large  $p_T$  jet is another typical process with the small momentum transfer; therefore a phenomenological parton fragmentation model is essential for the complete modeling of the four jets production.

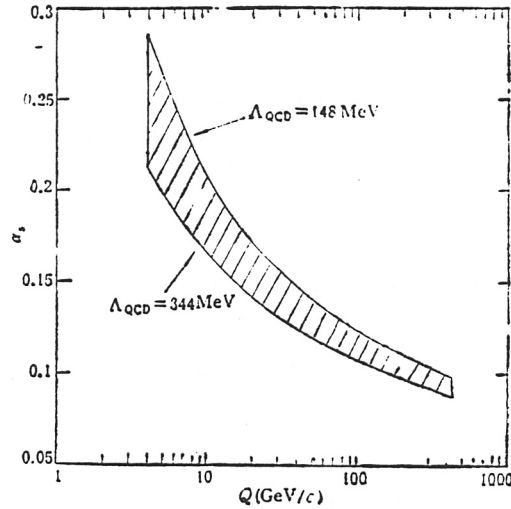


Fig. 1

The running of the strong coupling constant over the energy scales. The solid area indicates the uncertainty corresponding to the error of the measurement of  $\alpha_s(M_Z)$ .

The present paper is arranged as following: the large  $p_T$  jet production cross section and the  $p_T$  distribution of the jets will be calculated in the second, third and fourth sections. The results will be compared with the data gotten from collider experiments for the determination and the configuration of the parameters in the model. A hadronization model which is adopted in the ultrahigh energy region will be built in the words of Monte Carlo simulation in Section 5. The simulation of  $e^+e^-$  collision at the energies from 14 GeV to 91 GeV will be compared with the data gotten from collider experiments for the determination of the parameters in the model. A model for the soft component of the interaction will be found elsewhere, which will be adopted to describe the fragmentation of beam and target jets.

## 2. pQCD QUARK-PARTON MODEL AT ULTRAHIGH ENERGY

According to the quark-parton model, the Lorentz invariant inclusive cross section of jet production

$$E \frac{d^3\sigma}{dp^3} (pp \rightarrow \text{jet} + X) = \sum_{a,b} \int dx_1 dx_2 f_{a/p}(x_1, Q^2) f_{b/p}(x_2, Q^2) \left[ \int \frac{d\hat{\sigma}}{d\hat{t}} \right]_{ab}, \quad (1)$$

and the invariant parton-parton cross section

$$\left[ \int \frac{d\hat{\sigma}}{d\hat{t}} \right]_{ab} = \frac{\alpha_s(Q^2)}{s} |\tilde{\mu}_{ab}|^2 \delta(\hat{s} + \hat{t} + \hat{u}), \quad (2)$$

in which, the square of the scattering amplitude of  $2 \rightarrow 2$  sub-process is directly calculated with pQCD, the summation runs over the all concerning flavors and the gluon. The inputs of the model included: 1) hadronic structure function  $f(x_i, Q^2)$  characterizing the initialization of the momenta of the partons, participating the hard scattering, and their evolution before scattering. They are obtained by fitting the DIS data; 2) running coupling constant  $\alpha_s(Q^2)$ , which is measured by  $e^+e^-$  colliding experiments at

various scales; 3) unique expression of the momentum transfer  $Q$ , i.e., the evolution parameter, for different channels. There exist several expressions for  $Q$  in the references, e.g.,  $Q^2 = p_T^2$ ,  $Q^2 = (p_T/2)^2$  or  $Q^2 = \hat{s}\hat{t}\hat{u}/(\hat{s}^2 + \hat{t}^2 + \hat{u}^2)$ . The different expression for parameter  $Q$  will cause the corresponding uncertainties in the calculation. In practice, the parameter  $Q$  and their configuration will be fixed according to the consistence of the calculated results with the experimental data.

At ultrahigh energy, the domain of the quark-parton model of the 4-jet production is bounded by the geometry scaling. Integrating Eqs. (1) and (2) over the 3-momentum, one gets the exclusive cross section of the jet production

$$\begin{aligned}\sigma_{jet}^{pp}(\sqrt{s}) &= \frac{1}{2} \sigma(pp \rightarrow \text{jet} + X) \\ &= \frac{\pi}{s^{3/2}} \int_{x_1^{\min}}^{x_1^{\max}} d\eta dp_T dx_1 e^{\eta} \alpha_s(Q^2) \Sigma / x_1^2,\end{aligned}\quad (3)$$

in which,  $\Sigma = \sum_{a,b} f_{a/p}(x_1, Q^2) f_{b/p}(x_2, Q^2) |\tilde{\mu}_{ab}|^2$ ,  $\eta = -\ln \tan \frac{\theta}{2}$  is the pseudorapidity of the

outgoing parton,  $x_1^{\min} = x_1 e^{\eta} / (2 - x_1 e^{-\eta})$  is determined by the conservation of 4-momenta of the partons participating the hard scattering,  $x_T = 2p_T/\sqrt{s}$  and  $p_T$  is the transverse momentum of the jet, the factor of 1/2 comes from the assumption of only two partons in the final states of the hard scattering. In Eq. (3), there will be a divergence if the minimal cutoff of the transverse momentum  $p_T^{\min} \rightarrow 0$ , i.e., the geometric scaling is violated. Usually, the too-large inclusive cross section implies that either the perturbative QCD becomes non-applicable or there exist more than two final partons produced in the hard scattering which is beyond the calculation assumption. There are two traditional treatments for the problem associated to the violation of the geometry scaling. One is setting a relative high  $p_T$  cutoff to ensure the perturbative QCD being applicable, the other is to keep the  $p_T$  cutoff as low as possible, and consider that the final state of the hard scattering is consisted of multiple mini-jet with relative low  $p_T$ . In our question, we are only concerned the phenomena with extremely large apparent transverse momentum, therefore there is sufficient reason to assume that such mini-jets with small  $p_T$  in final state have no contribution to the very large apparent transverse momentum phenomenon in cosmic ray emulsion chamber experiments. A quite high  $p_T$  cutoff is set in our calculation, i.e.,  $p_T^{\min} = 4 \text{ GeV}/c$ . It is obvious that this is a very convenient treatment, because the final state always consists of two jets, and one need not worry about the violation of the geometric scaling. However, this simplicity of treatment is conditional. What we have paid is that the domain of the model is limited. Since the cross section of the jet production increases more rapidly with the interaction energy than that of proton-proton inelastic scattering, the geometric scaling will finally be violated as the interaction energy increase to a critical value,  $\sqrt{s_c}(p_T^{\min})$ . Fortunately, the critical energy reaches 22 TeV in proton-proton center of mass system corresponding to the  $p_T^{\min} = 4 \text{ GeV}/c$ . It is much higher than the working energy region of the cosmic ray emulsion chambers in practice.

### 3. RUNNING COUPLING CONSTANT AND STRUCTURE FUNCTION OF PROTON

The newest measurement [6] of the strong coupling constant at CERN LEP is

$$\alpha_s(M_{Z'}) = 0.118 \pm 0.008, \quad (4)$$

in which  $M_{Z'}$  is the mass of  $Z^0$ . According to the solution of renormalization group equation, the



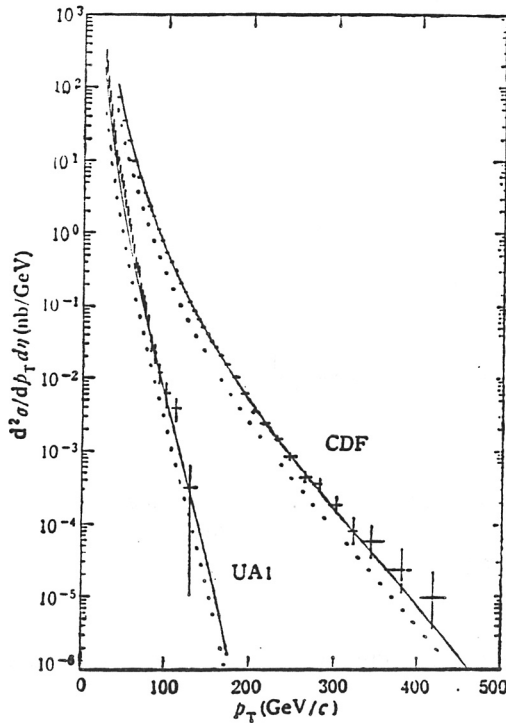


Fig. 2

The inclusive cross section of jet production in  $p\bar{p}$  versus transverse momentum of jets.

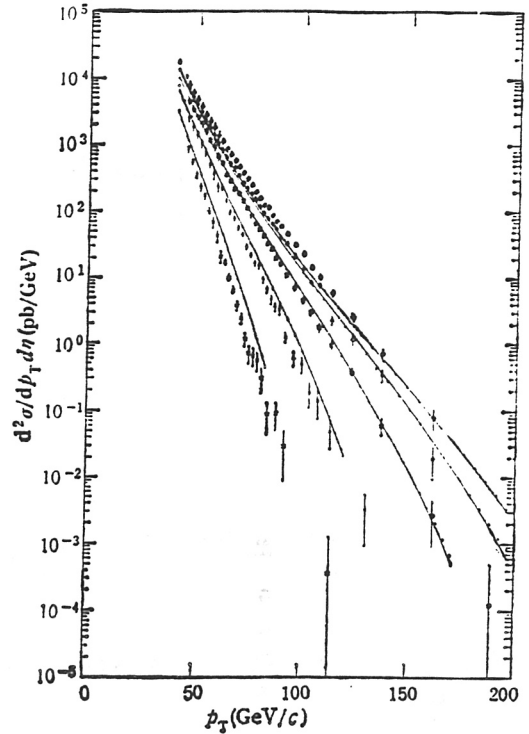


Fig. 3

The inclusive cross section of jet production in several pseudorapidity windows in  $p\bar{p}$  scattering. UA2 data:  $\circ$ :  $0.0 < \eta < 0.4$ ,  $\diamond$ :  $0.4 < \eta < 0.8$ ,  $\square$ :  $0.8 < \eta < 1.2$ ,  $*$ :  $1.2 < \eta < 1.6$  and  $\times$ :  $1.6 < \eta < 2.0$ .

running behavior of the coupling constant like

$$\alpha_s(Q^2) = 12\pi / (33 - 2n_f) \ln(Q^2 / \Lambda_{\text{QCD}}^2) \quad (5)$$

Since there is no terms  $O(\alpha_s^3)$  in our calculation, the running of the coupling constant is independent of the scheme of the renormalization. However, the evolution of the initial parton is not independent of the scheme of the renormalization. Therefore, for the sake of consistency, the  $\overline{\text{MS}}$  scheme of the renormalization is selected. Furthermore, in order to simplify the calculation, the heavy flavors are neglected in our model because their contribution is two orders smaller than that of the light sea quarks in proton, i.e.,  $n_f$  is taken as 3. From (4) and (5), the QCD scale is determined as

$$\Lambda_{\text{QCD}} = (246 \pm 98) \text{ MeV} \quad (\overline{\text{MS}} \text{ scheme}) \quad (6)$$

Corresponding to the uncertainty of the QCD scale shown in Eq. (6), the running behavior and the uncertainty of the strong coupling constant is shown in Fig. 1.

The structure function of proton is selected as the parametrization done by Marfin and Tung [7], which covered the most of DIS data and Drell-Yan process data. The sources of the data and a global analysis in the various schemes of the renormalizations are stated in detail in [7]. Many of the parametrizations are compared with each other. A parametrization, so-called S -  $\overline{\text{MS}}$ , of the structure

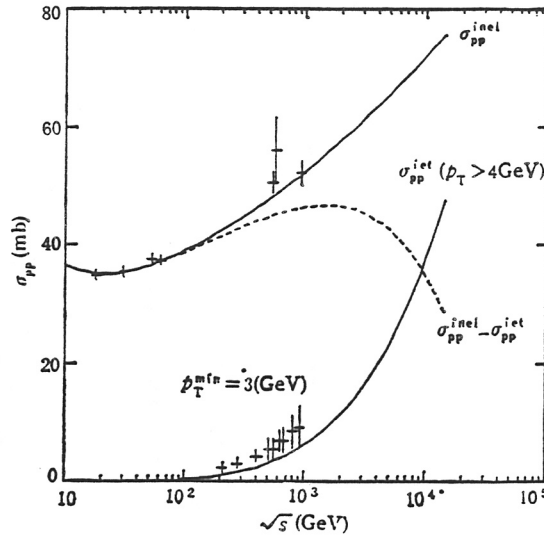


Fig. 4

The cross section of inelastic and jet production of  $p\bar{p}$  scattering versus center of mass energy of  $p$  and  $\bar{p}$ . The dashed curve refers to the cross section of soft component of  $p\bar{p}$  scattering.

function whose gluon distribution is the "hardest" among all of the parametrizations is selected in our calculation.

#### 4. JET PRODUCTION IN PROTON-PROTON COLLISION

In order to construct the framework of the model mentioned above and to study how to determine reasonably the parameters and their configuration as mentioned in Sections 2 and 3, the  $2 \rightarrow 2$  parton elastic scattering are calculated under the leading order approximation. The square of the invariant scattering amplitudes and the Mandelstam variables within them can be found in [8]. The inclusive transverse momentum distribution of jets, which can be directly compared with the data obtained in the collider experiments, is gotten by integrating Eqs. (1) and (2) over the pseudorapidity as,

$$\left. \frac{d^2\sigma}{dp_T d\eta} \right|_{\eta=\eta_0} (pp \rightarrow \text{jet} + X) = \frac{1}{\Delta\eta} \frac{2\pi\alpha_s^2(Q^2)}{\sqrt{s}^3} \int_{\Delta\eta} \int_{x_1^{\min}} d\eta dx_1 e^{\eta} \Sigma/x_1^2, \quad (7)$$

where  $\Delta\eta$  is the pseudorapidity interval centered at  $\eta_0$ . The comparison of the calculating results and the UA1 data [9] ( $\sqrt{s} = 546$  GeV,  $|\eta| < 0.7$ ), as well as the CDF data [10] ( $\sqrt{s} = 1.8$  TeV,  $0.1 < |\eta| < 0.7$ ) are shown in Fig. 2. The solid and dashed curves indicate the calculating results corresponding to the two parameter configurations, i.e.,  $Q^2 = (p_{T/2})^2$ ,  $\Lambda_{\text{QCD}} = 344$  MeV and  $Q^2 = (p_{T/2})^2$ ,  $\Lambda_{\text{QCD}} = 150$  MeV, respectively. It is easy to see that the difference between the two cases is smaller than a factor of 2, and the calculating results of first parameter configuration are closer to the data.

The  $p_T$  distribution of jets in several pseudorapidity windows are measured by UA2 ground [11], which reflect indirectly the angular distribution of jets. The calculation is consistent with the data quite well as shown in Fig. 3. Except for the effect of the different parameter configuration, the influence

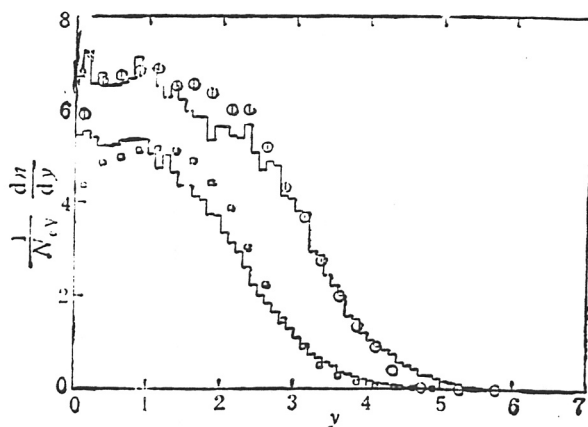


Fig. 5

The rapidity distribution of secondary hadrons in  $e^+e^-$  collision.  
 $\square$ : MARKII data,  $\circ$ : ALEPH data, histogram: the simulation.

of the different structure function is investigated. The calculating results with EHLQ [5] structure function are drawn in Fig. 3 with dashed curves. The two results are nearly identical to each other.

As mentioned in previous section, the geometric scaling can be conserved in a quite wide energy region under the assumption of only a pair of final jets produced in the hard scattering with the transverse momenta being higher than  $p_T^{\min} = 4$  GeV/c. The cross section of jet production calculated by means of Eq. (3), versus the center of mass energy, are drawn in Fig. 4. In the same figure are also plotted the inelastic cross section of  $p\bar{p}$ , the cross section of "pure soft" hadronic interaction which is determined simply by subtracting the cross section of jet production from that of inelastic scattering, and the data of cross section of jet production measured by UA1 [12]. According to the discussion in [13], the criteria used by UA1 for jets correspond to the  $p_T^{\min} = 3$  GeV/c. The critical energy, above which the geometric scaling would be violated, can be directly abstracted from this figure as about 22 TeV.

## 5. MONTE CARLO CODE OF HADRONIZATION

Based on the enormous amount of the data accumulated in the  $e^+e^-$  collisions with hadronic final states at several energies, the hadronization phenomenological models, represented by, e.g., Lund-PS [14] and HERWIG [15], have been well developed and have been able to entirely reproduce the experimental results. However, those models include a number of parameters, which are determined by fitting the data of  $e^+e^-$  experiments, so they usually cannot be directly adopted or extrapolated to the ultrahigh energy region. A phenomenological model, adopted mainly in the ultrahigh energy region, must be based on a clear physical picture, must have as few as possible parameters so that the uncertainties caused by the extrapolation to higher energy can be restricted in their minima, and must have a high operating speed on the computer. The last point is so important that one even has to give up a little high accuracy and entirety of reproduction of the experimental results for the high operating speed. After all, an independent fragmentation scheme of the jet whose dependence of the transfer momentum,  $Q^2$  characterizing the evolution of the parton is selected.

All the secondaries are assumed as pions because the emulsion chambers in cosmic ray experiments have no ability to identify the type of hadrons. The mass of the secondaries is taken as that of pions, i.e., 138 MeV. Under this assumption, the entire outgoing parton is simply taken as quark or gluon. A gluon immediately splits into a pair of a quark and an anti-quark whose energies

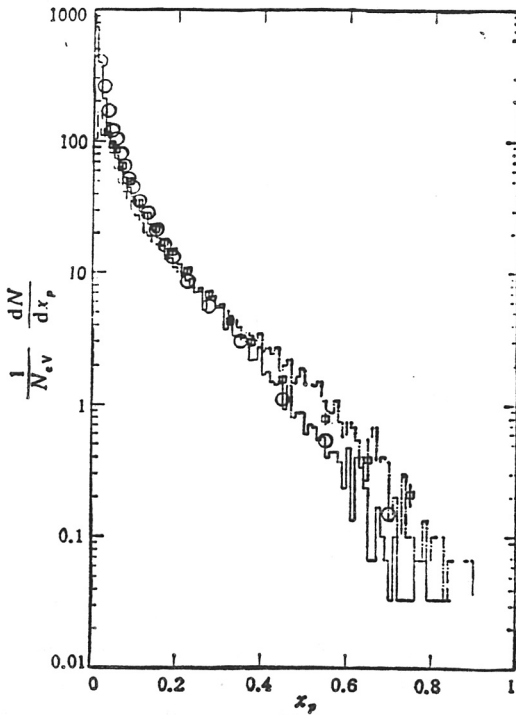


Fig. 6

The  $x_p$  distribution of secondary hadrons in the  $e^+e^-$  collision.  $\square$ : TASSO data,  $\circ$ : ALEPH data, histogram: the simulation at corresponding energies.

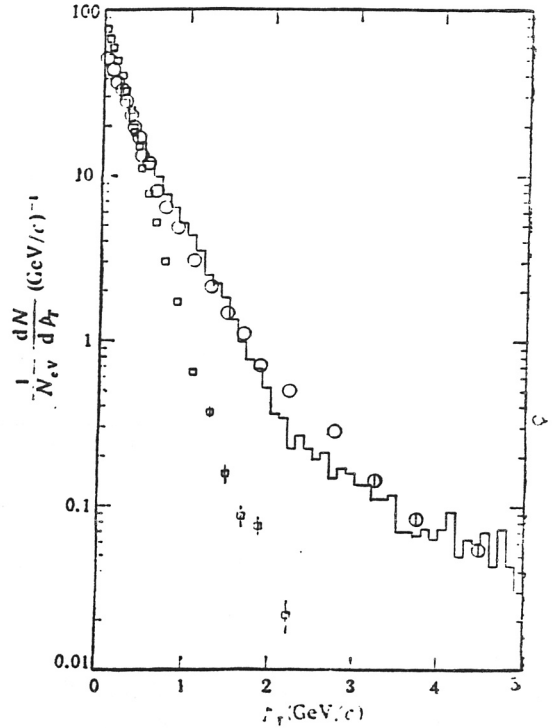


Fig. 7

The transverse momentum distribution of secondary hadrons in  $e^+e^-$  collision at LEP energy.  $\circ$ :  $p_T^{\text{in}}$ -distribution,  $p_T^{\text{out}}$ -distribution, histogram: simulation, which gives identical  $p_T^{\text{in}}$  and  $p_T^{\text{out}}$  distributions due to the neglect of the multi-jet production.

obey the following distribution [16],

$$f(x) = 3/2[x^2 + (1-x)^2], \quad (8)$$

where  $x$  is the fraction of energy of original gluon carried by the quark. The anti-quark carries the fraction  $(1-x)$  of the energy of the original gluon. The fragmentation of a quark in the final state of the hard scattering is divided into longitudinal and transverse fragmentation, in which the longitudinal and transverse momenta of secondary hadrons are determined respectively. At every step of the production of the secondary hadron, the produced hadron carries the amount of the light cone variables,  $W^+ = E + p_L$ , and the fraction of  $W^+$  carried by the specific hadron obeys the following distribution,

$$f(z) = (1 + c(Q^2))(1-z)^{c(Q^2)} \quad (9)$$

where  $z$  is the fraction of light cone variable as  $W_{\text{hadron}}^+/W_{\text{parton}}^+$ . The transverse momentum of the secondary hadron is defined in such a frame whose  $z$ -axis orientates the parton's momentum and its magnitude distributes as a Gaussian which standard deviation correlates to the longitudinal

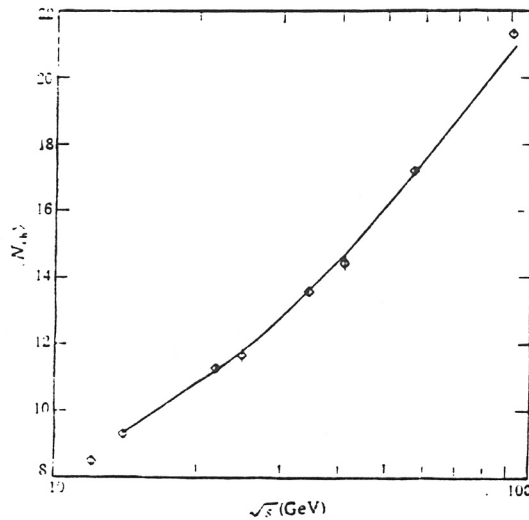


Fig. 8

The average multiplicity of the charged secondary hadrons in the  $e^+e^-$  collisions versus energy. The data taken from the TASSO, MARKII, TRISTAN and LEP exp. and the line indicates the simulation.

fragmentation as follows,

$$\sigma_{PT} = \begin{cases} \sigma_0(Q^2) - 0.7 + 0.7(z/z_1)^3 & (z < z_1) \\ \sigma_0(Q^2) & (z_1 < z < z_2) \\ \sigma_0(Q^2) \exp\{-2(z - z_2)\} & (z > z_2) \end{cases} \quad (10)$$

In Eq. (10) the parameters are determined by fitting the  $e^+e^-$  data as  $z_1 = 0.15$ ,  $z_2 = 0.55$ , and  $\sigma_0$  as well as  $C(Q^2)$  in Eq. (9) are both the functions of transfer momentum,  $Q$ , characterizing the evolution of the final state partons of the hard scattering. After releasing a hadron, the remnant parton has the light cone variable of  $(1 - z)W^+$  and the transverse momentum which is same as that of hadron's in the magnitude but in inverse direction. Then rotate all the momenta of both the hadron and the remained parton into the frame which  $z$  axis is in the direction of the original parton momentum. The whole process are iterated until the light cone variable of the remnant parton,  $W^+$  becomes smaller than two times pion mass. This means the remnant parton is not able to release any new hadrons. The multiplicity of secondary hadrons is controlled by all the parameters mentioned above, and is consistent with the data.

The forward and the backward partons are independently fragmented by means of the procedure described above. The 4-momentum conservation is ensured by implementing the procedure suggested by Ali *et al.* [17]. Using the difference of the summations of the longitudinal momenta of the forward and the backward secondary hadrons,  $\Delta Q$ , as well as the summation of the energy of all the hadrons,  $\Sigma E_H$ , to make up a parameter  $\beta = \Delta Q / \Sigma E_H$  as a Lorentz boost parameter. Then boost all the hadrons into a new frame, which is believed as the actual center of mass system of the initial parton-parton system. The 3-momentum is conserved. Then, the momentum of each hadron will be scaled up or down so that the ratio

$$\left[ \sum_{(\text{Hadrons})} (m_x^2 + \alpha^2(p_L^2 + p_T^2))^{\frac{1}{2}} - 2E_{\text{jet}} \right]^{\frac{1}{2}} / 2E_{\text{jet}} \quad (11)$$

is controlled to be smaller than  $10^{-3}$ , in which the factor  $\alpha$  is obtained by search scheme. After doing this, the total energy will conserve with the uncertainty of less than  $10^{-3}$ .

All the parameters in the model are determined by fitting the  $e^+e^-$  data at several collider energies and then are extrapolated to the ultrahigh energies. By fitting the rapidity distribution of the hadrons of MARKII (29 GeV) [18] and ALEPH (91 GeV) [20], the fraction of momentum,  $x_p$  distribution of TASSO (22 GeV) [19] and ALEPH [20], as well as the transverse momentum distribution measured by ALEPH [20], the parameters and their dependence of energy are fixed as

$$c(Q^2) = 0.055 + 0.874 \ln E_{\text{jet}}, \quad (12)$$

in which  $\sigma_0(Q^2)$  is a slowly varying function of  $\ln E_{\text{jet}}$  between 0.08–0.28 GeV/c, the parameter  $Q$  characterizing the evolution of the original partons is taken as the center of mass energy of the pair of the partons, i.e.,  $2E_{\text{jet}}$ . The comparisons of the simulating results with experimental data are shown in Figs. 5–7. As seen in Fig. 8, the average multiplicity of charged secondaries increases with the square of the logarithm of the energy [21], which is consistent with the data of [18–20].

## 6. SUMMARY

Based on the models described above, a generator of the hard component of proton-proton inelastic scattering is constructed. Firstly, the cross sections of jet production are calculated with Eq. (3) at the center of mass energy from 80 GeV to 14 TeV. The occurrence of jet production is sampled with the probability of its cross section ratio to the inelastic scattering; the type of the sampled jet is determined according to the relative fraction of cross sections of quark or gluon among the cross section of jet production. The pseudorapidity and the transverse momentum of the jet are then sampled according to their distributions, respectively. Calling the fragmentation procedure described in Section 5, and transforming all the hadrons into the center-of-mass system of initial proton-proton scattering, the jet production process is completed. The complete simulation of a non-diffractive proton-proton interaction can be carried out by combining the generator of hard component and another generator described in [5], which is for the simulations of the soft component of the  $p\bar{p}$  scattering and the fragmentation of the beam and target jets.

The model built here reasonably reproduces the experimental results at the collider energies with less parameters (only 5, except for that appearing in the structure functions), and smoothly extrapolated into the ultrahigh energy region of  $\leq 10^{17}$  eV. It is applicable to predicting or explaining the results of the cosmic ray emulsion chamber or extensive air shower experiments. Moreover, the generator including only the pQCD under LLA provides a framework for exploring the new physics at ultrahigh energy. For example, it have been used for investigation of the possible effects of the compositeness of quarks on the analysis of the multi-cluster phenomena in emulsion chamber experiments, or it can be adopted to investigate the possible ultrahigh energy gamma-nucleus interaction mechanism for the explanation of the strange phenomena in the extensive air shower experiments of searching for ultrahigh energy gamma sources, and so on.

Because of the lack of a more basic theory describing the processes with small momentum transfer, one has to describe such a complicated interaction with an approximate and phenomenological model. The predictions of the model could not be consistent with the data in all aspects. In the current version of the model, there are explicit defects, i.e., it cannot reproduce measured multiplicity distribution. The main reason for this is that the fluctuation in the hadronization is not sufficiently

considered, e.g., the parton shower has not been taken into account for the evolution of the final states of the hard scattering. Another defect is the violation of geometric scaling at the extremely high energy. After all, it is presumably an applicable tool for exploring the new physics in ultrahigh energy cosmic ray physics.

## REFERENCES

- [1] C. M. C. Lattes *et al.*, *Phys. Rep.*, **65** (1980), p. 151.
- [2] Ren Jingru *et al.*, *Phys. Rev.*, **D38** (1988), p. 1404.
- [3] Ren Jingru *et al.*, *High Energy Phys. and Nucl. Phys.* [Chinese edition], **13** (1989), p. 77.
- [4] Q. Q. Zhu *et al.*, *J. Phys.*, **G16** (1990), p. 295.
- [5] Cao Zhen and Ding Ling kai, *High Energy Phys. and Nucl. Phys.* [Chinese edition], **18** (1994) p. 990.
- [6] Siegfried Bethke, CERN-PPE/91-36.
- [7] J. G. Marfin and W. K. Tung, *Z. Phys.*, **C52** (1991), p. 13.
- [8] R. P. Feynman, R. D. Field and G. C. Fox, *Phys. Rev.*, **D18** (1978), p. 3320.
- [9] UA1 Coll., G. Arnison *et al.*, *Phys. Lett.*, **172B** (1986), p. 461.
- [10] CDF Coll., Fermilab-conf. 90/91-E.
- [11] UA2 Coll., J. Alitti *et al.*, *Phys. Lett.*, **257B** (1991), p. 232.
- [12] UA1 Coll., *Nucl. Phys.*, **B309** (1988), p. 405.
- [13] F. Halzen, Proc. 21st Int'l. Cosmic Ray Conf., Adelaide, **12** (1990), p. 101.
- [14] M. Bentsson and T. Sjostrand, *Phys. Lett.*, **185B** (1987), p. 435.
- [15] T. Sjostrand and M. Bentsson, *Comput. Phys. Comm.*, **43** (1987), p. 367.
- [16] G. Altarili and G. Parisi, *Nucl. Phys.*, **B126** (1977), p. 298.
- [17] A. Ali *et al.*, DESY Internal Report T-80/01.
- [18] Mark-II Coll., A. Pettersen *et al.*, *Phys. Rev.*, **D37** (1988), p. 1.
- [19] TASSO Coll., M. Althoff *et al.*, *Z. Phys.*, **C22** (1984), p. 307; TASSO Coll., W. Braunschweig *et al.*, *Z. Phys.*, **C45** (1989), p. 193.
- [20] ALEPH Coll., D. Decaph *et al.*, *Phys. Lett.*, **234B** (1990), p. 209.
- [21] May Coll., Y. K. Li *et al.*, *Phys. Rev.*, **D41** (1990), p. 2675; May Coll., H. W. Zhang *et al.*, *Phys. Rev.*, **D41** (1990), p. 737.